CNESOC FLIGHT DYNAMICS MONITORING AND COMMAND OPERATIONS DURING GALILEO FOC1 LEOP AND RECOVERY

Jorge Lopez Merida[(1)], **Livio Tucci** [(2)] , **Riccardo Di Corato** [(3)] , **Fernando Alonso Zotes** [(4)]
[(1)]*GMV @ESA/ESOC, Robert Bosch-Str. 5, Darmstadt, Germany, +49 6151 90 3343, Jorge.Lopez-Merida@esa.int*
[(2)]*SCISYS Deutschland GmbH @ESA/ESOC, Robert Bosch-Str. 5, Darmstadt, Germany, +49 6151 90 2053, Livi.Tucci@esa.int*
[(3)]*SCISYS Deutschland GmbH @ESA/ESOC, Robert Bosch-Str. 5, Darmstadt, Germany, +49 6151 90 4207, Riccardo.Di.Corato@esa.int*
[(4)]*Terma GmbH @ESA/ESOC, Robert Bosch-Str. 5, Darmstadt, Germany, +49 6151 90 2654, Fernando.Alonso.Zotes@esa.int*

Abstract: *This paper presents the highlights of the CNESOC attitude monitoring and command generation Flight Dynamics (FD) team operations during Galileo Full Operational Capability (FOC) 1 LEOP and the following recovery phase.*

Keywords: *Solar array deployment, Sun pointing phase monitoring, on board orbit calculator, initial pressurant mass error impact on PVT method, manoeuvre calibration.*

1. Introduction

In the context of Galileo FOC, the CNESOC team is a result of collaboration between CNES and ESOC centres with members from both establishments. As part of it the flight dynamics monitoring and command generation team is responsible for monitoring the spacecraft attitude dynamics and generating commands related to the AOCS subsystem. In addition, at ESOC a test and validation team performs parallel monitoring and validation of all the FD operational products, using independent tools, in order to assure the safety and quality of operations.

The first two Galileo FOC satellites were launched on August 22nd 2014. Unfortunately, due to a launcher anomaly, they were injected in a severely non-nominal eccentric orbit.
The latter was so far off from target that the nominal operational orbit could not be reached, with the fuel loaded on-board. Too low temperatures in the solar array (SA) deployment mechanism initially also prevented the deployment of one SA wing for each of the two spacecraft, leading to a series of contingency operations to achieve as soon as possible their successful deployment. The failed SA deployment could be observed by FD based on the estimated versus expected spacecraft inertia matrix.

After the deployment was accomplished, both spacecraft were kept in a safe Sun-pointing attitude for an extended period, while a new achievable target orbit was defined.

In the recovery phase, a series of orbit control manoeuvres (OCM) were performed in order to increase the perigee altitude such that the Earth sensor could operate normally, targeting at the same time an orbit somehow suitable for the Galileo constellation in terms of resonance and ground coverage. Before that, a series of analyses were done to ensure the spacecraft operability in an orbit far from the design specification, especially in terms of the on-board orbit propagator, conceived for orbits with very low eccentricity. The consumption of a very significant part of the available propellant to achieve the new target orbit gave FD the chance

to observe the spacecraft propulsion system during most of its life cycle, close to end-of life conditions. The mass consumption predictions had to be refined in order to ensure the overall feasibility of the manoeuvre strategy, taking into account in particular the thruster off-modulation observed during manoeuvres. Comparisons between the fuel book keeping respectively based on pulse counting and PVT methods showed increasing discrepancies as the propellant was being consumed. This lead into an analysis showing the effect of initial pressurant mass errors in the PVT method predictions.

This paper describes these activities and analysis performed by the telecommand and attitude monitoring team during the LEOP and recovery phase.

2. Solar array deployment and angular momentum

2.1. Introduction and analysis

Under nominal LEOP conditions, Galileo satellites switch to Solar Acquisition Mode (SAM) shortly after separation. The two solar panels, stowed during the launch, shall deploy during SAM along spacecraft local frame axes +Y and -Y. This manoeuvre is simple, however critical for the whole life of the mission, as the solar panels are the source of electrical power for the Galileo payload. For this reason, the deployment takes place only after assuring the satellite angular rates are below a threshold of 6 degrees per second. Nominal angular rates after separation are below 2 deg/s around satellite Z-axis, below 4 deg/s around X-axis and below 4 deg/s around Y-axis, thus a nominal magnitude higher than 6 deg/s is not expected. Once the spacecraft is in SAM, angular rates damping control activates if necessary till the rate magnitude is below the aforementioned 6 deg/s. Only within this threshold shall the controller send a request to start the solar panels deployment mechanism. This is done by the arming and firing of nominal and redundant HRDMs, simultaneously for both solar arrays – however, these “thermal knives” might not respond immediately, leading to a small time gap between the two deployments-.

As a result of the deployment of the solar arrays, the angular rates are expected to decrease due to the Newton’s third law of motion: the angular momentum $\boldsymbol{L}$ in a rotating body is rigorously constant if no external torques are applied to the body. Indeed, the constant angular momentum $\boldsymbol{L}$ is proportional to the tensor of inertia $\boldsymbol{[I]}$ and the angular rate $\boldsymbol{\omega}$:

$$\bar{L} = [I]\bar{\omega} \tag{1}$$

The moment of inertia respect to the rotation axis a is:

$$I_a = \int_{S/C} r_a^2 dm = \int_{body} r_a^2 dm + \int_{\substack{solar \\ arrays}} r_a^2 dm \tag{2}$$

As shown in equation (2), symmetrical changes in mass respect to the rotation axis a (in example, due to the simultaneous deployment of two geometrically symmetrical solar arrays) may not change the direction of the rotation, however will change the moment of inertia I_a , respect to the rotation axis a:

$$\Delta I_a = \int_{\substack{solar \\ arrays}} \Delta r_a^2 dm \tag{3}$$

If the rotation axis a is a main inertia axis, the component of the L vector along axis a is:

$$L_a = I_a \omega_a \tag{4}$$

According to equation (4), the increase in the moment of inertia as described in (3) shall lead to a decrease of the angular rate around axis a. Given no external torque, and provided the rotation is around a main inertia axis so its direction remains constant, the value of L_a in equation (4) does not change before and after the deployment of the solar arrays, yielding to:

$$\omega_{a,aft} = \frac{I_{a,bef}\omega_{a,bef}}{I_{a,aft}} \tag{5}$$

where the suffices *bef* and *aft* denote the status of the different magnitudes before and after the deployment, respectively. Equation (5) specifies how the change in the moment of inertia affects the rotation rate.

Although the conditions of the Galileo spacecraft do not rigorously match the symmetrical requirements for equations (4) and (5) , because the nutation effects due to time gap between the two deployments, and the multi-axis components of the rotation in body frame, the reasoning above is still applicable: a change in the deployment status of the panels shall be observed through the change in the angular rate which, besides nutational oscillations, should match quite well the predicted values based on the moments of inertia before and after deployment.

Based on this idea, it was possible to compute three different estimators for the angular momentum. An angular momentum computed assuming solar arrays are not deployed, $L_{est,stowed}$; an angular momentum assuming only one solar array is deployed, $L_{est,1\text{-}deploy}$; and an angular momentum calculated assuming both arrays are deployed, $L_{est,deploy}$. The inertia matrix for each deployment status is based on data provided by the manufacturer of the spacecraft (OHB System AG). The angular rate is provided by AOCS telemetry. The estimators are computed according to equation (1). Due to the symmetry of the solar arrays in the spacecraft frame, $L_{est,1\text{-}deploy}$ can be used for estimations regardless of which of the two arrays has been deployed.

Due to the conservation of angular momentum, the value of L before, during and after deployment should remain constant. The estimated values, however, are based on different inertia matrices, hence yielding to:

$$L_{est,stowed} < L_{est,1-deploy} < L_{est,deploy} \tag{6}$$

Whilst the solar arrays are stowed, the angular momentum L shall match $L_{est,stowed}$. Once one of the solar panels is deployed, the value of $L_{est,1\text{-}deploy}$ after one array deploys should match the value of $L_{est,stowed}$ before deployment. Similarly, $L_{est,deploy}$ shall become the best estimation of the constant value of L after total deployment. As pointed out above, equations (4) and (5) are not longer strictly applicable due to nutation effects, however the monitoring of the angular rate is still an important clue, so an unexpected behaviour of the three L_{est} estimators may lead to conclude the deployment failed, from the point of view of Flight Dynamics. Other teams may come to the same conclusion by analysing the electrical output of the arrays.

2.2. Observations during LEOP

The evolution of the angular momentum of spacecraft 261 (aka. Galileo-5) can be seen in Fig. 1, together with the angular rates and the thrusters actuation. Note the results are plotted respect to on-board time, which was not synchronized to UTC until later on. The Galileo L3 mission separation took place nominally on 2014/08/22 at 16:15:07.5 UTC. Nutation effects can be slightly appreciated, however no major differences respect to a rotation around a main inertia axis. The start of the solar arrays deployment for 261 occurred around 2014/08/21 at 12:52:44 (on-board time) - matching an "artifact" peak in angular momentum -, and was completed at around 12:56:16 – matching the start of the thrusters, used for Sun acquisition -. The results strongly suggested one of the solar panels was stowed. Indeed, $L_{est,deploy}$ after deployment should match the value of $L_{est,stowed}$ after separation. Instead, it was $L_{est,1\text{-}deploy}$ that matched the initial value of $L_{est,stowed}$.

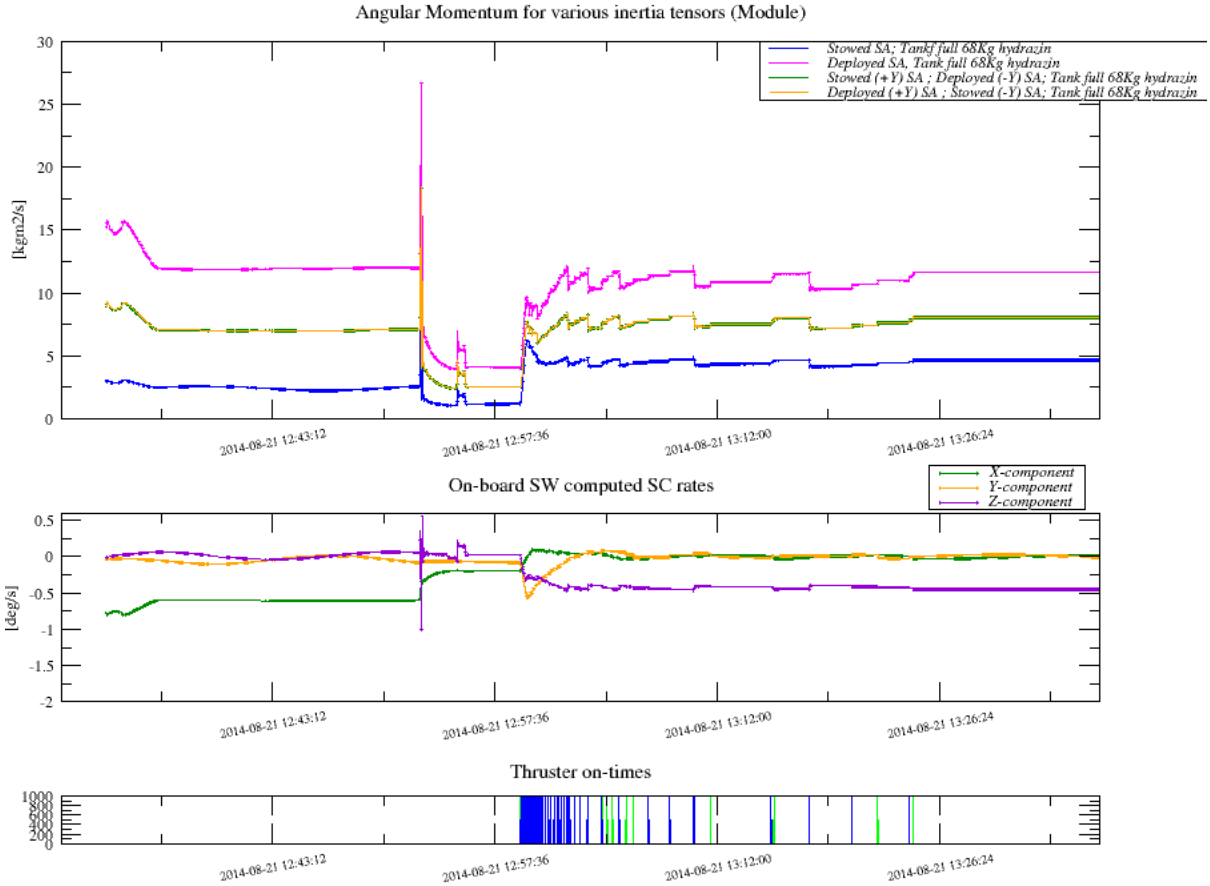

Figure 1. Monitoring spacecraft 261 during first solar array deployment attempt

Similarly, the evolution of the angular momentum of spacecraft 262 (aka. Galileo-6) can be seen in Fig. 2, together with the angular rates and the thrusters actuation, in on-board time. The solar arrays deployment for 262 occurred on 2014/08/21 from 12:45:27 to 12:58:32 (on-board times). The results again suggest one of the solar panels was stowed, according to the values of $L_{est,deploy}$ and $L_{est,1\text{-}deploy}$ immediately after deployment.

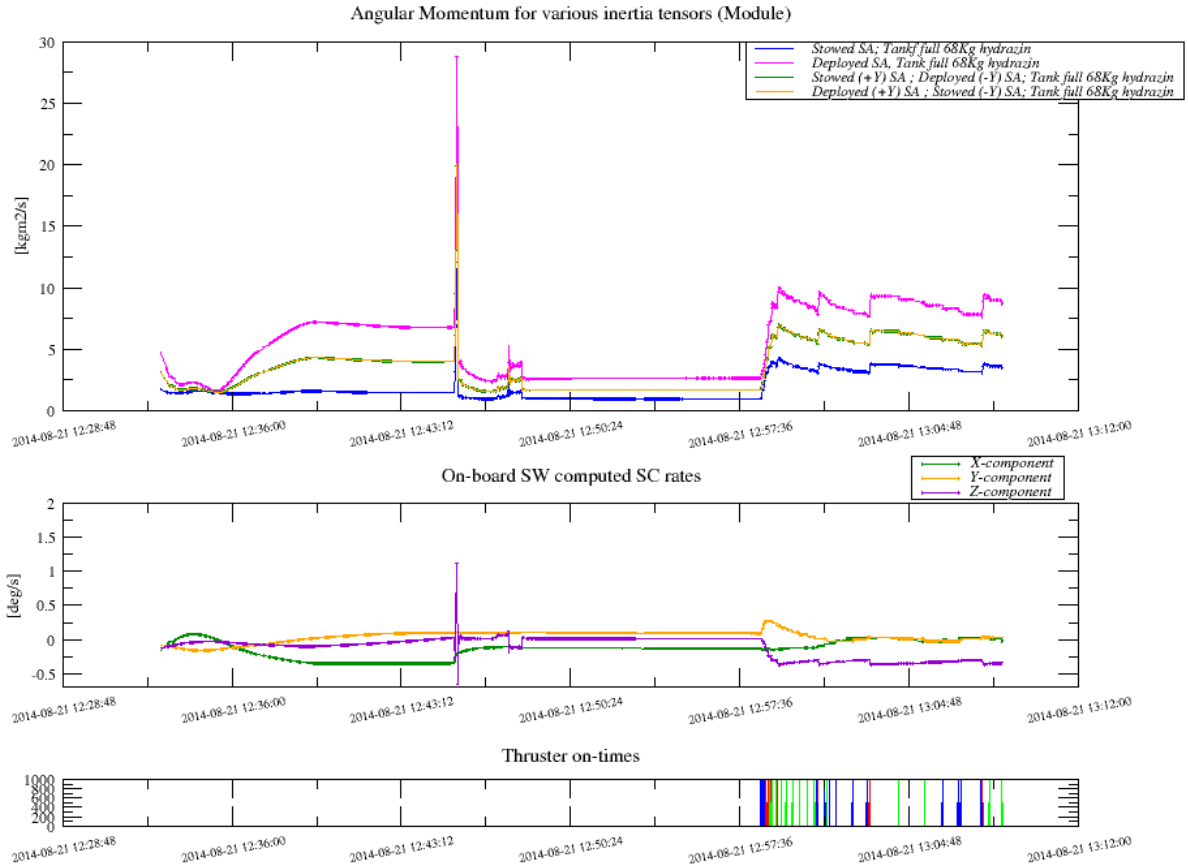

Figure 2. Monitoring spacecraft 262 during first solar array deployment attempt

2.3. Recovery procedure

It was believed the reason for the failure of the deployment of one solar panel in each spacecraft was related to thermal issues. The HRDMs or "thermal knives" release the solar arrays by applying heat, however this process may fail if the appropriate temperature cannot be achieved – for instance, if the side of the solar array is not illuminated by the Sun -. Indeed, for both spacecraft, only the panel in the side of the Sun deployed successfully: -Y for 261 and +Y for 262.

A procedure to deploy the stowed panels was implemented, consisting on 3-axis-stabilizing the spacecraft, prior to rotating around the X-axis (using reaction wheels) until the stowed panel is illuminated, and firing the HRDMs afterwards. The rotation was split into several smaller slews. The angular momentum is null during the activation of the reaction wheels for 3-axis stabilization, but we can observe a transitory effect during slews and an "artifact" peak during deployment of the stowed solar array.

The first procedure was simulated beforehand on 2014/08/25 for spacecraft 262. The procedure consisted on three 10 degree slews. On the same day, the procedure was executed. The monitoring of the spacecraft during the three slews and the -Y solar array deployment (followed by a final slew manoeuvre, to achieve the nominal attitude) are shown in Fig. 3 (note the different time scale in the plot of the angular momentum). Eventually, after the successful deployment, the attitude control based on thrusters was active again.

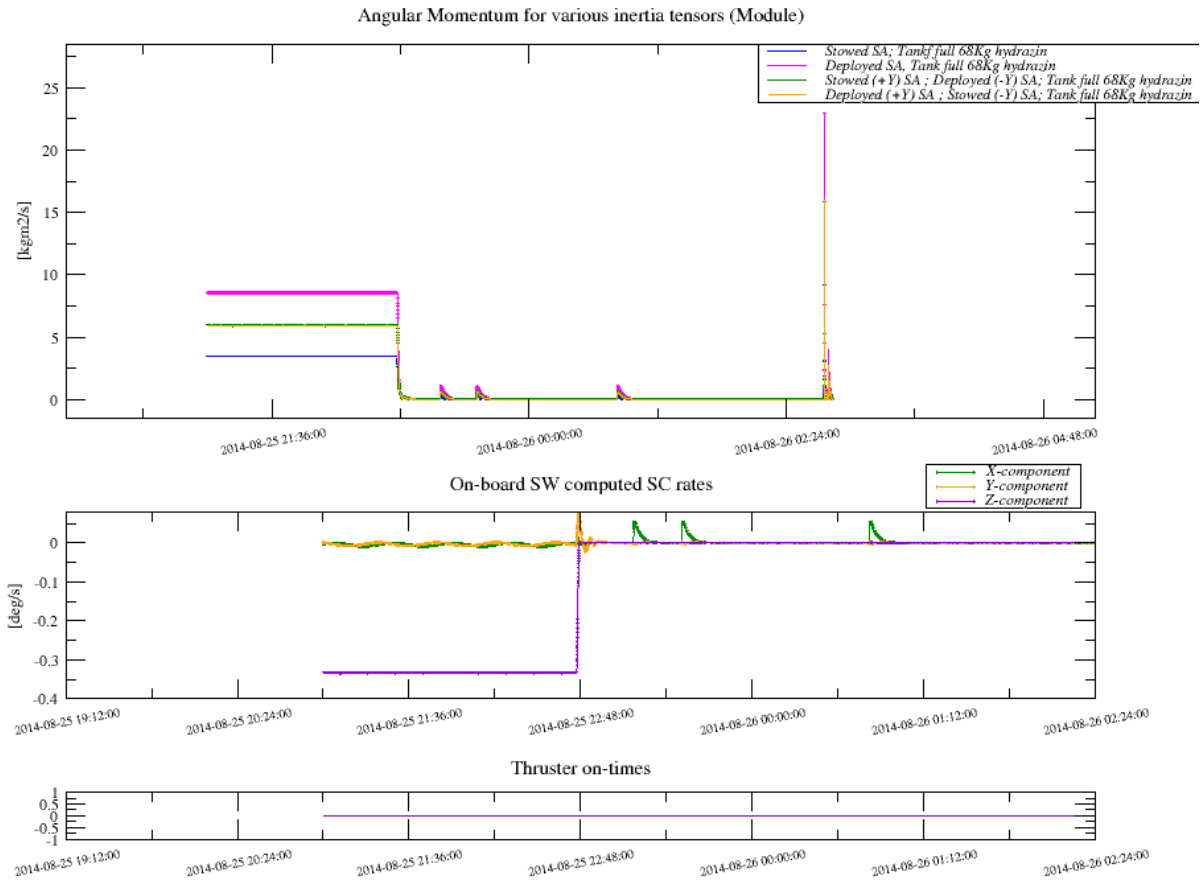

Figure 3. Monitoring 262: three-axes stabilization, three slew manoeuvres, -Y solar array deployment and last slew manoeuvre

Another simulation took place on 2014/08/27 for spacecraft 261 and consisted on three slews of 10, 10 and 5 degree respectively. On the same day, the procedure was executed, however skipping the last slew due to concerns about the temperature of the stowed solar panel. The monitoring of the spacecraft during the two slews and the +Y solar array deployment (followed by two slews to achieve nominal attitude) is shown in Fig. 4. After the successful deployment, the attitude control based on thrusters was active again, as shown in the third plot.

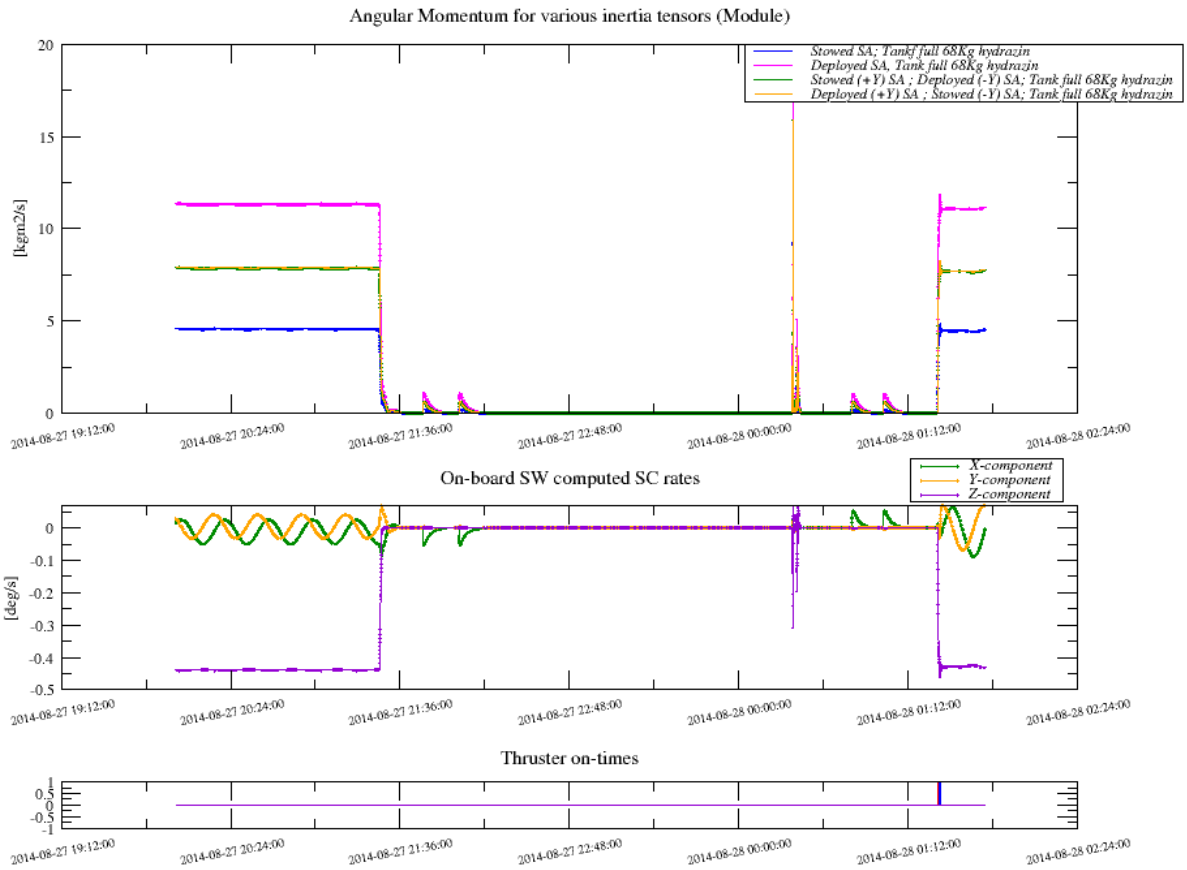

Figure 4. Monitoring 261: three-axes stabilization, two slew manoeuvres, -Y solar array deployment and last two slew manoeuvres

3. SAM and baby-sitting monitoring

The spacecraft Sun Acquisition Mode (SAM) is entered after INIT mode completion. The final goal of this mode is to acquire a safe Sun pointing attitude (-$\boldsymbol{Z_{sc}}$ to the Sun) with a predefined spin rate of about less than 0.4 [deg/s] around that very axis, being therefore spin-stabilized, with the solar arrays (SA) continuously charging. The spacecraft can autonomously stay in SAM for unlimited period without need of any ground support. Transition from SAM to higher modes is not autonomous and needs to be initiated by ground. SAM makes use of Coarse Sun Sensors (CSS) and gyroscopes (GYR) as sensors and thrusters as actuators. Sun direction in spacecraft frame is estimated making use of CSS data nominally blending it with GYR data to increase accuracy. Spacecraft rates are estimated using GYR data. Attitude control torques are nominally provided by the thrusters.

After the activation of all the necessary AOCS units, the on-board controller reduces the spacecraft rates below a certain threshold for the stowed configuration. SA deployment is then triggered without any active attitude control. After the successful completion of SA deployment, if necessary, spacecraft rates are once again reduced below a second threshold for the deployed configuration. Only at this point the controller start the slew to acquire the Sun on the $-\boldsymbol{Z_{sc}}$ axis with a constant spin rate about it. Once this is achieved, the spacecraft enters a regime of passive attitude stabilization with a dead-band control on the Sun average deviation from the $-\boldsymbol{Z_{sc}}$ axis. The latter two phases are called Sun acquisition and Sun Maintenance phases.

Sun acquisition is initially entered from the rate damping phase when the spacecraft rate is lower than 2 [deg/s] . The initial Sun acquisition finishes when the control keeps the average Sun deviation from the $-\boldsymbol{Z_{sc}}$ axis less than 5 [deg] average over 1000 [s] , and the target angular rate around $-\boldsymbol{Z_{sc}}$ is reached. Once the Sun pointing is acquire it starts the Sun maintenance phase, where there is no active attitude control until the average Sun deviation from the $-\boldsymbol{Z_{sc}}$ axis is more than 25 [deg]. In case the depointing becomes larger than 25 [deg] the Sun pointing is corrected until the depointing reduces again to 5 [deg]. The de-pointing is achieved by activation of pair of thrusters at a given time.

The controller controls the three spacecraft axes in a sequential way: $\boldsymbol{X_{sc}}$, $\boldsymbol{Y_{sc}}$, $\boldsymbol{Z_{sc}}$.

For $\boldsymbol{X_{sc}}$ and $\boldsymbol{Y_{sc}}$ control a controller based on phase plane principles is used, controlling both corresponding spacecraft angles and rates around zero, ensuring $-\boldsymbol{Z_{sc}}$ Sun pointing. For $\boldsymbol{Z_{sc}}$ control is only rate control. Actuation is triggered whenever angular rate around $\boldsymbol{Z_{sc}}$ is deviating more than 20% from the target rate.

The overall attitude control concept just above described is illustrated hereafter in the Fig. 5, showing real telemetry data from spacecraft 261 in the time period between 2014.09.02 and 2014.09.03.

The time span has been selected to show a typical transition from SAM Sun maintenance to SAM Sun acquisition and back.

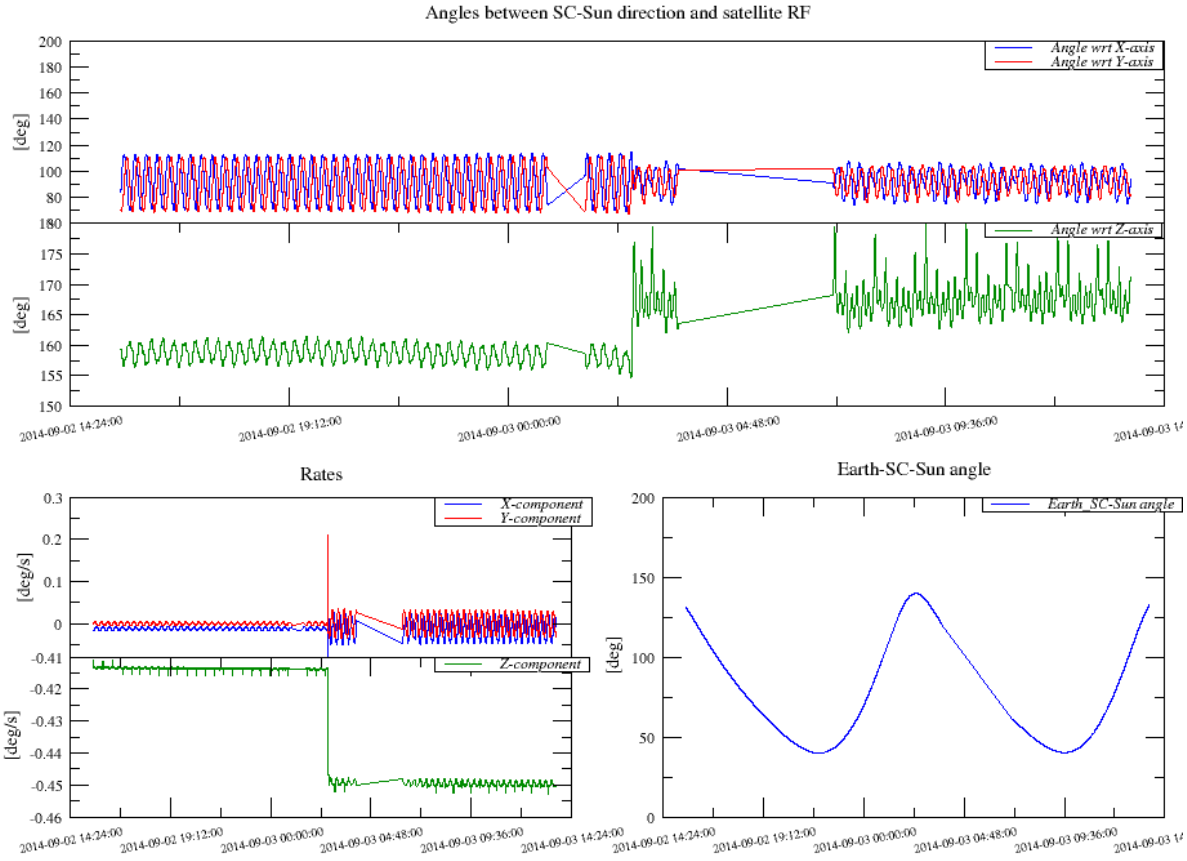

Figure 5. Spacecraft 261 real telemetry data during SAM Sun maintenance and Sun Acquisition

Focusing hereafter on Galileo FOC L3 operations, both spacecraft were handed over from CNESOC to GCC on 2014.09.26, stable in SAM mode, generating power from the SA and charging the platform batteries.

From LEOP end to handover to GCC the following activities where performed by CNESOC Flight Dynamics, namely:

- monitor AOCS being always SAM
- monitor Sun direction in spacecraft frame (estimated by CSS and GYR data)
- monitor spacecraft rates (estimated by GYR data)
- monitor on-board estimated orbit state with respect to the one computed from FD operational orbit
- monitor thruster activity
- perform propellant consumption book keeping whenever thruster activity is observed

For both spacecraft, after the mission control team managed to finally deploy the not deployed SA on each spacecraft during LEOP, a quite long period starting from then and extending past the handover to GCC was spent in SAM Sun maintenance, with periodic autonomous switch to SAM Sun acquisition and back, as just described above. Later on, it was decided to perform recovery operations for the two spacecraft in sequence, first 261 and then 262.

Spacecraft 261 was in SAM maintenance with both SA deployed from 2014.08.28 to 2014.11.03 for approximately 67 days, until it was finally commanded to Nominal (NOM) mode, in order to subsequently perform the first test orbit control maneuver two days later on 2014.11.05. During this interval 367 [g] of propellant have been used for attitude control for an average propellant consumption of approximately 5.5 [g/day].

Spacecraft 262 was instead in SAM maintenance with both SA deployed from 2014.08.26 to 2015.01.17 for approximately 144 days, until it was finally commanded to Nominal (NOM) mode, in order to subsequently perform the first test orbit control maneuver two days later on 2015.01.19. During this interval 656 [g] of propellant have been used for attitude control for an average propellant consumption of approximately 4.6 [g/day].

The propellant evolution during SAM for spacecraft 261 and 262 is shown hereafter in Fig. 6 and Fig. 7 respectively. Each data point corresponds to a fuel book keeping calculation performed by CNESOC shortly after the autonomous actuation took place on-board: the epochs protocolled in the graphs more precisely correspond to end time of each Sun acquisition phase. From the graph, it can be noticed that for both spacecraft the actuations are quite well regularly spaced among each other. The gap in data points corresponds to the period whereby the spacecraft were already handed over to GCC, pin which CNESOC did not perform any fuel book keeping. That was done in GCC. CNESOC did receive a propellant mass consumption update, just prior the start of the recovery operations in 2014.11 and 2015.01 respectively: those are the last data points in the two graphs.

Also a linear propellant consumption trend is clearly observable for both spacecraft as an expected consequence to the periodic nature of the disturbance torques forcing the spacecraft attitude dynamics during the passive period of Sun maintenance.

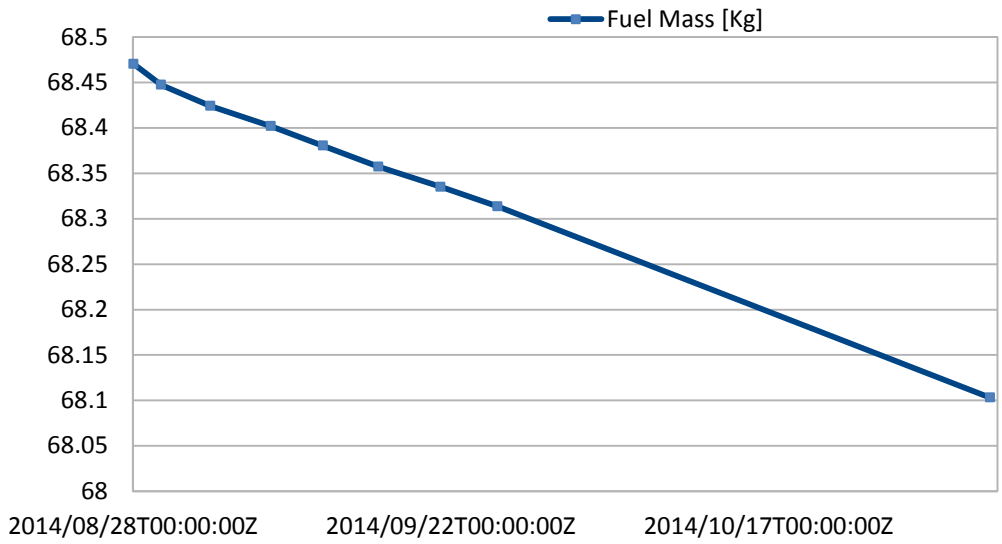

Figure 6. Spacecraft 261 propellant mass during SAM

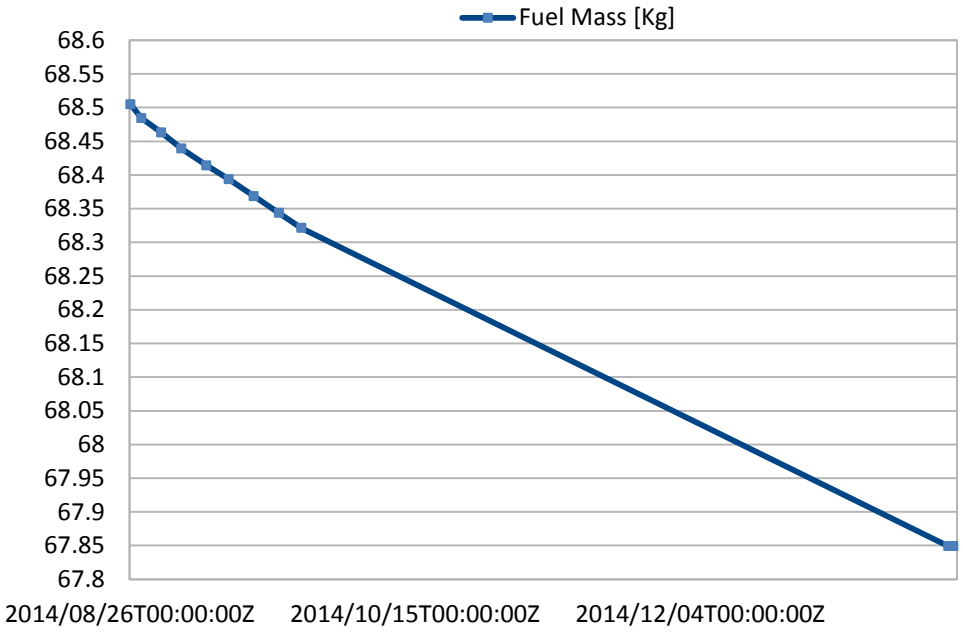

Figure 7. Spacecraft 262 propellant consumption during SAM

Overall, both spacecraft spent quite a considerable amount of time in SAM before the recovery operations started, showing a very good and stable behavior in term of attitude estimation, attitude control and thruster performance and propellant consumption.

4. On-board orbit calculator behaviour

The Galileo FOC spacecraft computes its own position, as well as the Sun and Moon position, using the "on-board orbit calculator" software module. The implemented model is a simple linear propagation, requiring the following input from ground:

- Osculating Keplerian elements with respect to ECI J2000 reference frame at a reference time t_0. The sixth commanded Keplerian element is the mean anomaly.

- Keplerian elements decay parameters between t_0 and t_1. These parameters are Keplerian elements time derivatives, computed based on the Keplerian elements values at t_0 and t_1, taking into account that angles are defined in the [0 360] deg range. The time interval between t_0 and t_1 is by default set on ground to seven days.

The on-board orbit calculator parameters are contained in a FD command, nominally foreseen to be uplinked, during LEOP, after every orbit determination and before/after every manoeuvre. It is a key command, since it affects, among other things, the spacecraft accuracy in predicting Earth sensor blinding and in computing the yaw steering law. The FD system has been designed to take into account the spacecraft position as computed on-board when modelling the predicted spacecraft attitude.

When a new on-board orbit calculator command is generated, the discrepancy between the propagated spacecraft position with respect to the FD orbit file is computed for a time interval of seven days. If the established check thresholds are exceeded (in terms of discrepancy at uplink time, during the propagation interval and jump with respect to the previous on-board orbit calculator parameters), the command is rejected and the discrepancies are investigated. The FD check tool emulates the on-board software algorithm when computing the spacecraft position from the commanded parameters.

A large amount of testing has been performed on this command with successful outcome during Flight Dynamics system tests and simulations, based on a number of nominal and contingency orbits. Figure 8 represents the propagation error for spacecraft 262 for the on-board orbit calculator command generated during the FD operational system initialisation, based on the nominal injection orbit. The along-track error reaches a maximum of about 5 km in the middle of the propagation interval.

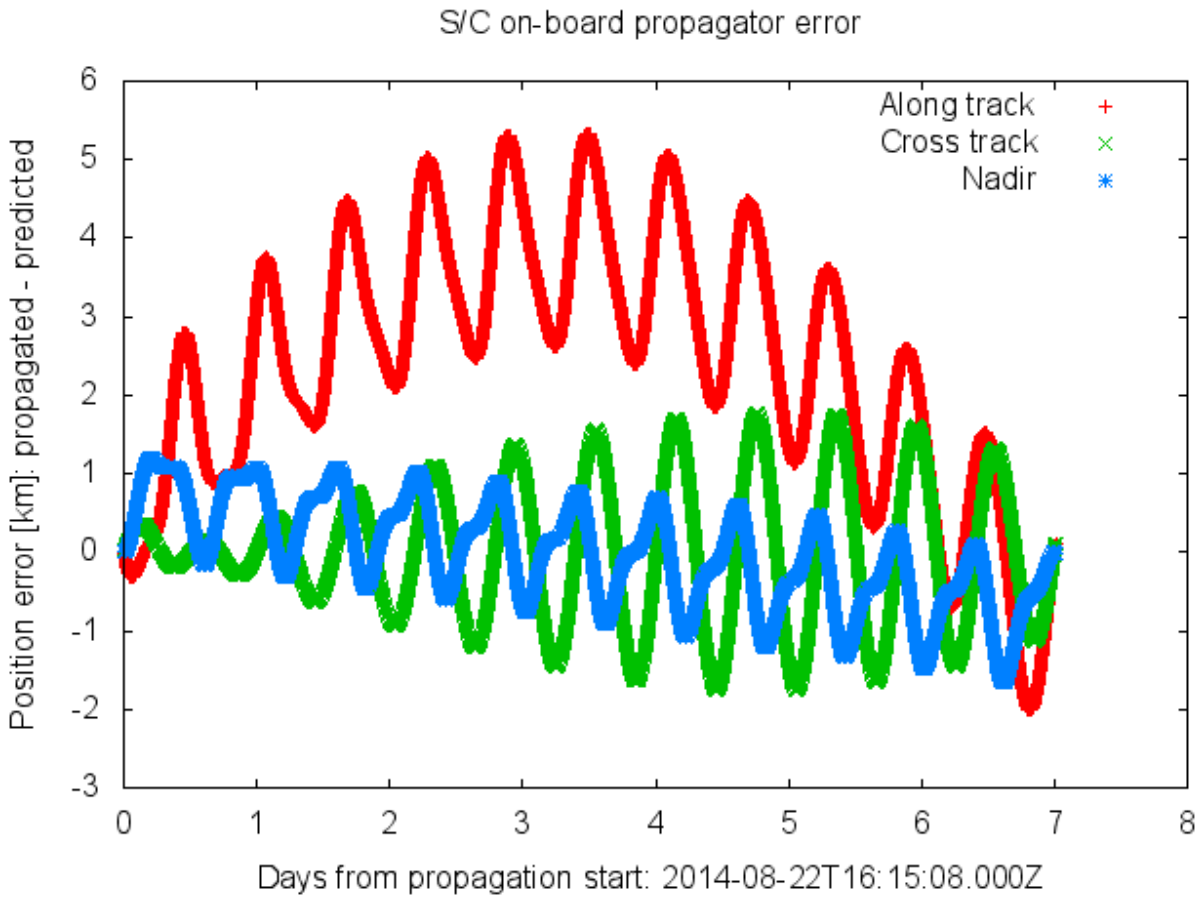

Figure 8. On board propagator position error with nominal injection orbit

During LEOP, at around MET 22:00, Flight Dynamics was requested to generate the first on-board orbit calculator command based on the determined orbit, for spacecraft 262. The command was not intended to be uplinked (the spacecraft does not use the orbit calculator as long as it remains in Sun Acquisition Mode), but to be fed to the simulator in order to evaluate its effect. The command was generated and checked following nominal procedures. While the check of Sun and Moon on-board calculator parameters passed without showing any anomaly, the spacecraft on-board propagation error with respect to Flight Dynamics orbit file showed the unexpected trend represented in Fig. 9.

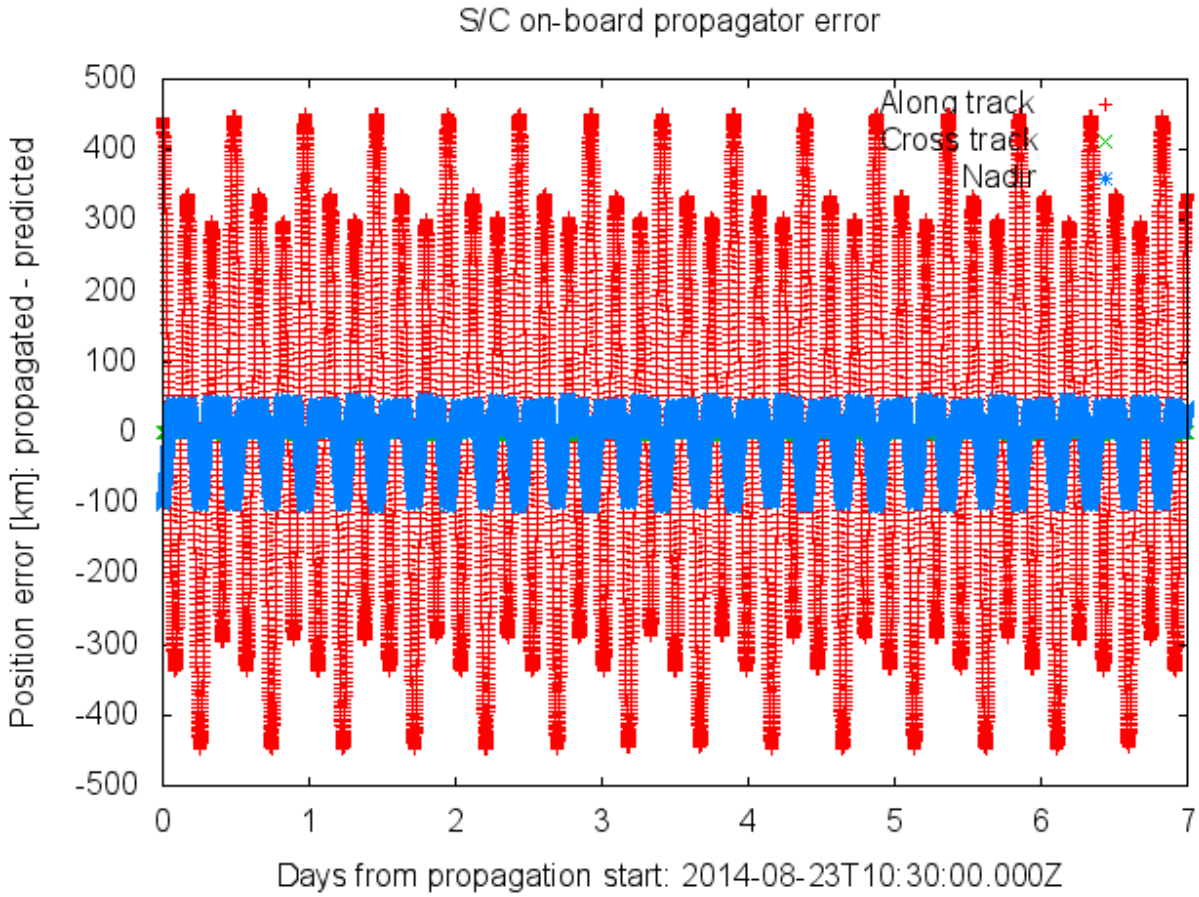

Figure 9. On board propagator error with initial injection orbit

All error components have a harmonic trend, whose period corresponds to the orbital period of the determined orbit (about 12 hours). The largest error component is the along-track one, reaching maxima of about 450 km. The error is already close to the maximum at the start of the interval, and does not noticeably increase during the propagation interval. For comparison, the command acceptance threshold at interval start is 10 km along-track.

The error trend immediately suggested that the root cause of the anomaly may not be the Keplerian elements propagation algorithm, but the on-board software conversion from Keplerian elements to position vector, which had never been tested by Flight Dynamics with a highly eccentric orbit. An investigation was carried out during a LEOP shift, in order to fully understand the anomaly. Code inspection of the on-board orbit calculator command check tool, which emulates the on-board software algorithms, revealed that the conversion from mean anomaly to true anomaly is performed using the following approximated formula:

$$\nu = M + 2 \cdot e \cdot sin(M) + \frac{5 \cdot e^2 \cdot sin(2 \cdot M)}{4} \qquad (7)$$

where ν is the true anomaly, M the mean anomaly and e the eccentricity. This approximated formula is accurate for low eccentricity orbits such as the nominal Galileo operational orbits, but not suited for highly eccentric orbits such as the one experienced during this LEOP. In order to verify that this approximate formula leads to the error reported by the command check tool, the true anomaly at command uplink time was computed both based on an accurate algorithm (using generic FD software) and on the approximated formula. The two

values differed by 0.93 deg which, converted to an orbit arc, resulted in a distance of 425.36 km, matching the command check tool results.

In addition, a small script was developed on the fly, which accesses the FD orbit file during one orbit revolution and computes the difference in true anomaly between accurate and approximate algorithms, and the corresponding position error. Results are shown in Fig. 10 and Fig. 11: the error is zero at perigee and apogee and maximum for true anomaly of 111 deg and 249 deg. The maximum error of 450 km previously found by the command check tool could be confirmed by the results of this script.

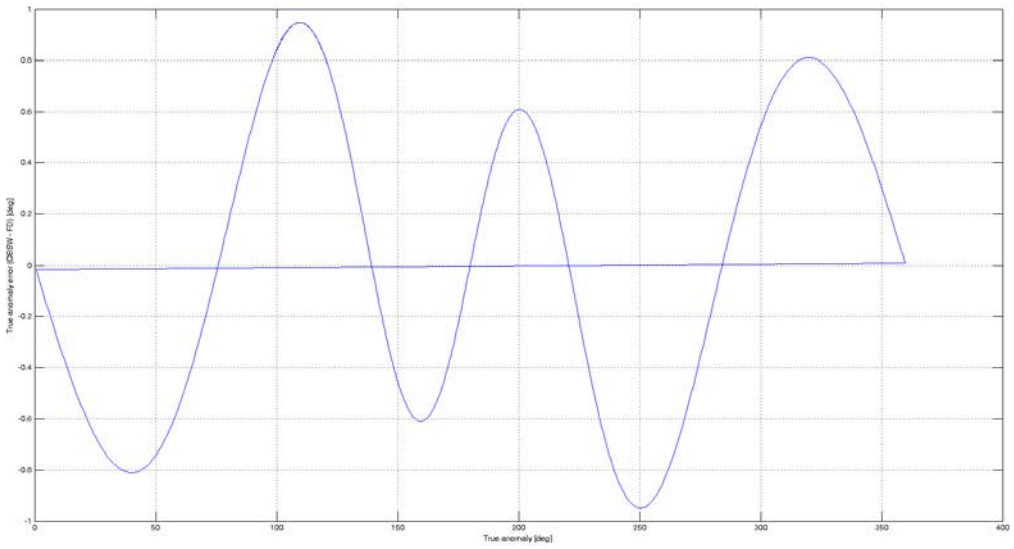

Figure 10. True anomaly difference On board SW .vs. FD orbit

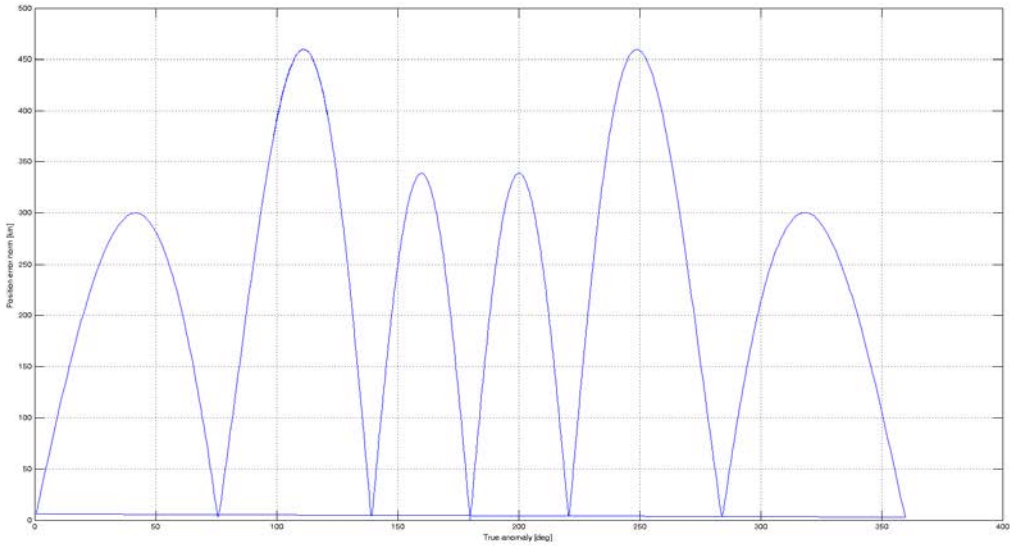

Figure 11. Position difference On board SW .vs. FD orbit

These results were shared with the Flight Control Team and Project Support Team. It was agreed that, given the nature of the discrepancy, no simple modification of the ground command could improve the accuracy of the orbital position computed on-board. In addition,

the Project Support Team verified that a position error of the observed magnitude would not cause major problems to the spacecraft once it would start using the on-board calculator in Earth Acquisition Mode and Normal Mode. Therefore, the option of patching the on-board software with a more accurate model was ruled out for the time being. Instead, it was agreed to generate a new command with a later execution time and uplink it, in order to verify that the on-board software computation of the spacecraft position matches the FD prediction and that no other unexpected effects occur.

The command was generated for spacecraft 262 with a reference time of 2014-08-23T19:10:00Z. The command check yielded similar results as the test command previously checked, with the difference that the initial along track error in this case was 111.167 km. This confirmed the results of the analysis: the initial error only depends on the S/C true anomaly at the command execution time, and does not affect the maximum error, which essentially depends on the orbit eccentricity.

The command was uplinked and executed on-board at 19:41:40Z. FD computed the expected along-track error at this time and obtained -169.33 km. The S/C position computed on-board (as received in TM) dropped from a very large value to the expected value, as confirmed by the FD monitoring plot showed in Fig. 12.

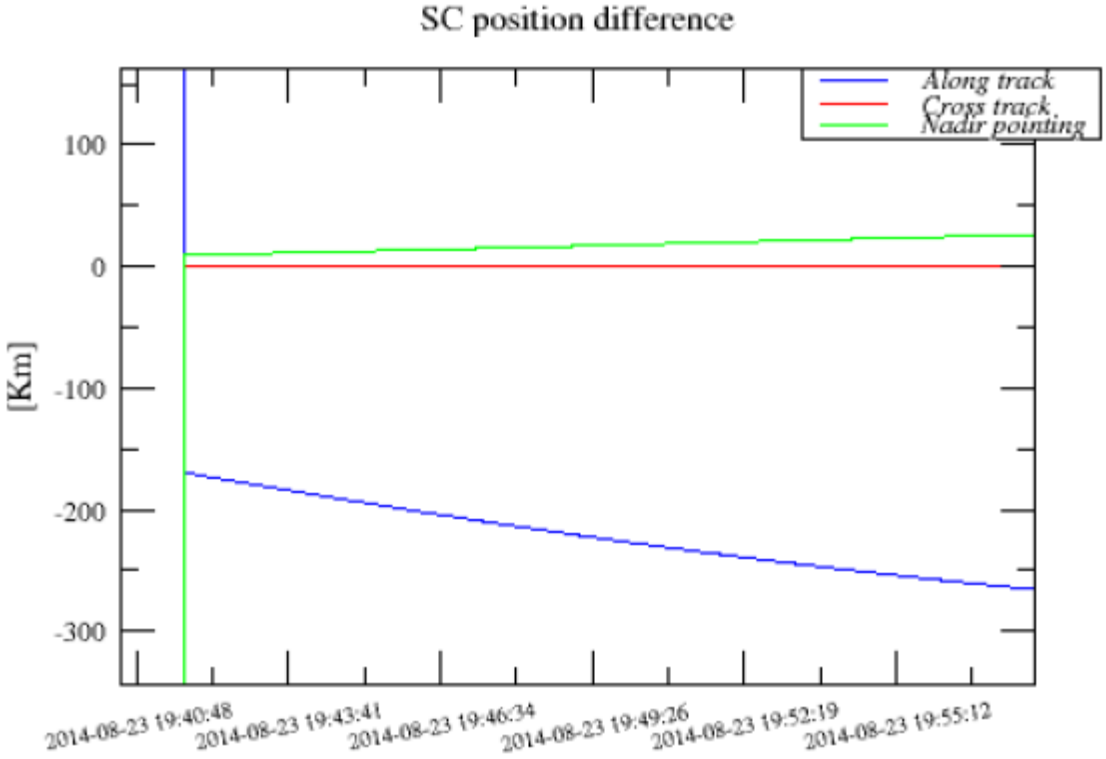

Figure 12. Monitoring of on board orbit update .vs. FD orbit

5. Long term on-board orbit calculator error prediction

On 2014-09-02, the spacecraft “babysitting” phase started, with an initially planned approximate duration of one month. During this phase, the S/C was left in Sun Acquisition Mode, spinning around its Z axis and executing isolated thruster pulses to correct the Sun pointing error.

Since no on-board orbit calculator command was planned to be generated during this phase, the command uplinked during LEOP on 2014-08-23 was checked again with respect to the current FD orbit and with an extended check interval, up to 2014-10-01. Results for S/C 261 are shown in Fig. 13. The maximum S/C along track error slowly increases during the check interval, but remains lower than 500 km. This shows that the effect of propagating outside the 7 days interval used to generate the command is minor compared with the error caused by the approximate true anomaly computation.

The Sun and Moon on-board orbit calculator long term plots showed no surprising trend: the error remains low during the first 7 days and increases immediately afterwards. The Earth-Sun vector angle error exceeds its threshold on 2014-09-15T02:31:00.000Z and increases up to a maximum of 0.06 degree at interval end. The Moon vector angle error exceeds its threshold on 2014-09-01T19:57:00.000Z and reaches a maximum of about 10 deg.

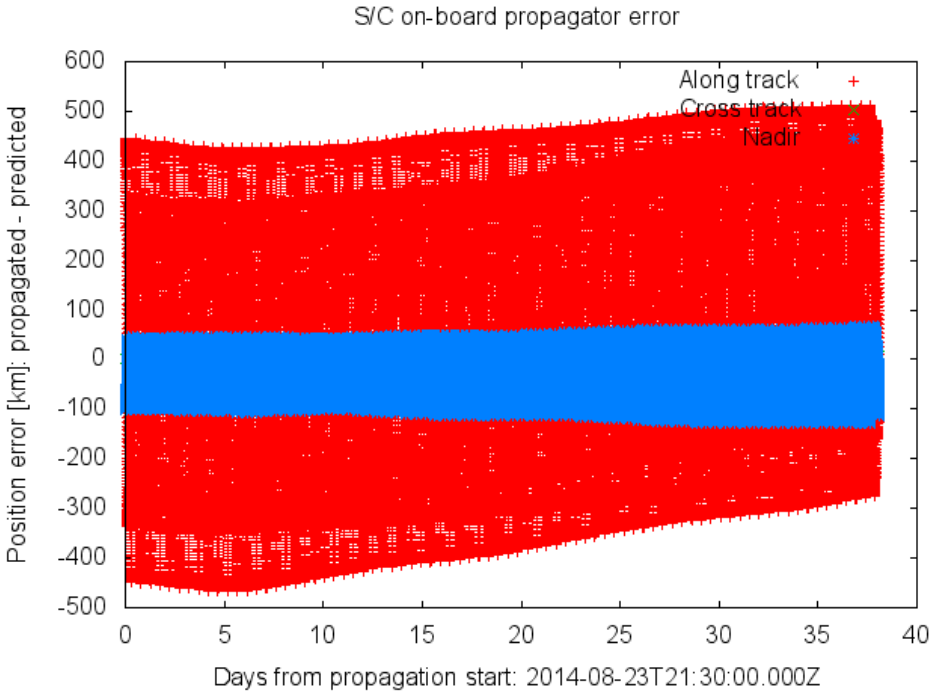

Figure 13. S/C on-board orbit position error

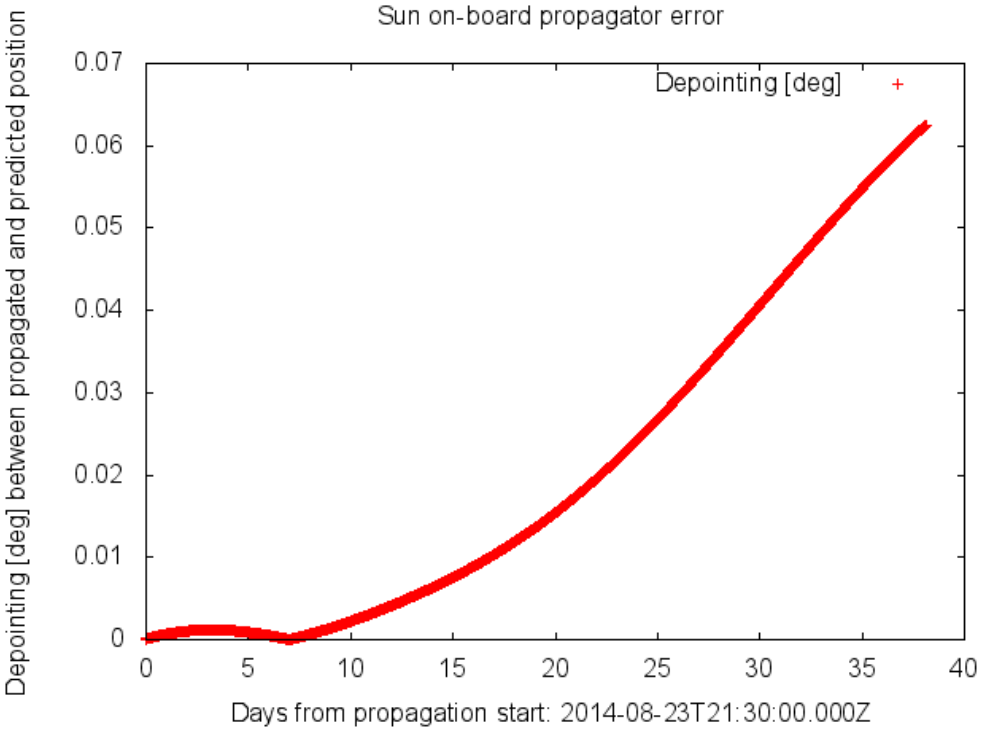

Figure 14. Depointing between propagated and predicted Sun position

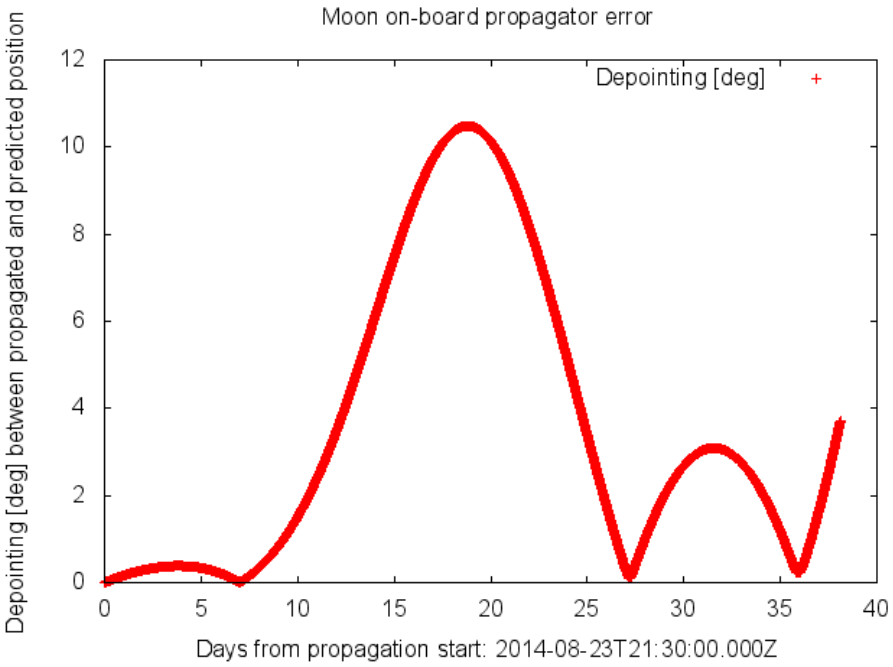

Figure 15. Depointing between propagated and predicted Moon position

6. Effect of initial pressurant mass error on the PVT method computation

The monitoring of the fuel mass consumption during manoeuvres and other thruster activities was done based on two different methods. First the fuel book keeping method, which estimates the fuel consumption monitoring the thruster activation and tank pressure, based on

the thruster modelling. And second the PVT model which evaluates the fuel mass in the tank at a specific point on time, based on the tank pressure and tank temperature measurements.

The PVT method evaluates the fuel mass in the tank computing the volume occupied by the propellant in the tank, which is the difference between the volume in the tank and the volume occupied by the pressurant. Both propellant and pressurant are separated by an elastic diaphragm, which also produces some gas due to some catalytic reactions along time. The propellant in this case is hydrazine, and the pressurant is Helium. And the hydrazine mass is then computed with the PVT method with the following equation:

$$m_{hyd\_pvt} = \rho_{hyd} \cdot \left[V_{tank} - \left(\frac{m_{He} \cdot R_{He} \cdot T_{hel}}{(P - P_{hyd\_vap}) \cdot 10^5} \right) - V_{gas} \right] \quad (8)$$

Where m_{hyd_pvt} is the hydrazine mass, ρ_{hyd} is the hydrazine density, V_{tank} is the current tank volume, P_{hyd_vap} is the hydrazine vapour pressure as a function of temperature, P is the current tank pressure, T_{hel} the current helium temperature, m_{He} is the helium mass, R_{He} is the Helium gas constant (2077 J/KgK), and V_{gas} is the gas volume volume generated by the tank diaphragm.

The volume of the tank slightly varies with pressure, with a value of 0.091815 m^3 at 1 bar. And the volume of gas generated by the tank diaphragm due a catalytic reaction is a function of time and other factors, which can be assumed negligible at the beginning of the mission.

During the Sun pointing and baby sitting phases the thruster activity was reduced to sporadic pulses to control the Sun pointing. The pressure in the tank was almost not affected by small firings, and only the variations of temperature in the tank due to thermic cycles produced much bigger changes of pressure than the ones produced by the decrease of pressure due to the firings, so that during this period only the fuel book keeping method was considered.

Later on, when the manoeuvre campaign started in the recovery phase, both methods were evaluated in parallel. But since the first manoeuvre there were significant discrepancies of fuel mass consumption between both methods, as can be observed in the following graph:

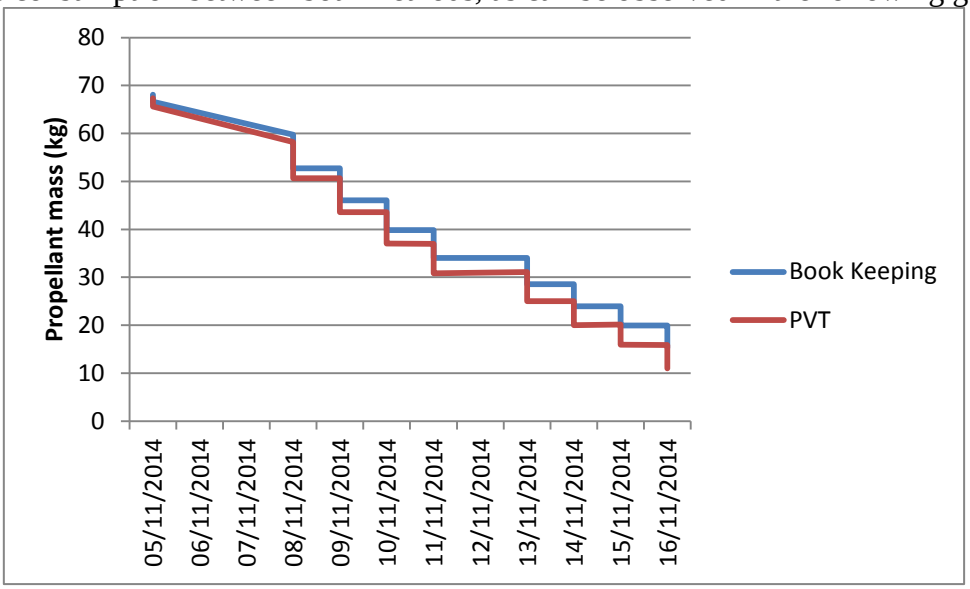

Figure 16. Propellant mass estimation book keeping .vs. PVT s/c 261

The blue line corresponds to the propellant mass estimated by the fuel book keeping method, and the red line the propellant mass estimated by the PVT method. In particular, for the first test manoeuvre the book keeping method estimated a mass consumption of 1.467 kg, while the PVT method estimated a mass consumption of 1.727 kilograms, a 18 % bigger.

This difference between both methods increased along time, as shown in the following plot, which represents the difference of mass in kg between the book keeping and the PVT.

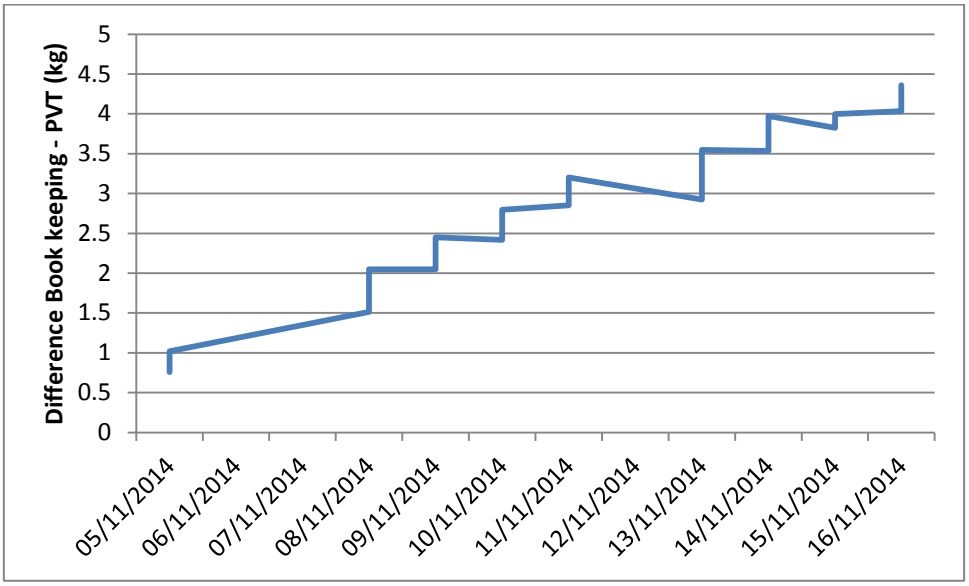

Figure 17. Difference in propellant mass between book keeping and PVT s/c 261

The fuel book keeping was selected then as reference for the fuel mass consumption, as it is considered more reliable than the PVT method in general from experience in other missions. However, following a conservative approach, the remaining fuel mass computed with the PVT method was used to estimate the remaining available delta-v. This had the following consequences:

- The target orbit had to be slightly changed with respect to the original plan as a fuel saving measure.
- Part of the fuel budget originally reserved to Safe Modes had to be used to acquire the target orbit, assuming the PVT method result to be correct.

Later analysis together with industry pointed that inaccurate values of the initial pressurant could result in inaccuracies in the PVT method. The initial pressurant mass was recomputed then based on initial filling conditions provided by industry, obtaining a value of 0.084366 kg, 5 grams different to the pressurant mass initially used (0.0898 kg) , or a 6 % different.

When recalculating the fuel mass for spacecraft 261 with this estimated pressurant mass the PVT method gave then a value of 15.729 kg, around 5 kg more fuel mass calculated before, which meant a 30% difference, and much closer to the book keeping estimation of 15.35 kg.

This showed that a small error in the initial pressurant mass can result in big errors in the PVT method. Furthermore this error increases as the fuel is being consumed, as the pressurant occupies more volume in the tank, and therefore has a bigger impact in the PVT.

As result of this, a better estimation of the initial pressurant mass was provided by industry. Another updated value of pressurant mass was used during the manoeuvre campaign for the spacecraft 262, with a significant improvement in fitting book keeping and the PVT methods.

7. Manoeuvre calibration

7.1. Calibration

In the context of the manoeuvre preparation and manoeuvre planning, a calibration factor was applied based on the efficiency observed in previous manoeuvres. This efficiency is evaluated for each manoeuvre based on the Delta V observed through the orbit determination:

$$\eta_{last\ manoeuvre} = \frac{\Delta V\ measured}{\Delta V\ expected} \tag{9}$$

And it was used to correct the calibration used for the preparation of following manoeuvres:

$$\eta_{manoeuvre(i)} = \eta_{last\ manoeuvre} \cdot \eta_{manoeuvre(i-1)} \tag{10}$$

This calibration was directly applied to the thruster model affecting the manoeuvre duration commanded to achieve certain Delta V.

During the manoeuvre campaign the calibration factor used resulted to be quite stable in time. In particular the initial calibration used was 0.95 in prevision of a 5 % off modulation. But in the end it resulted to stabilize in around 0.85 for both spacecraft.

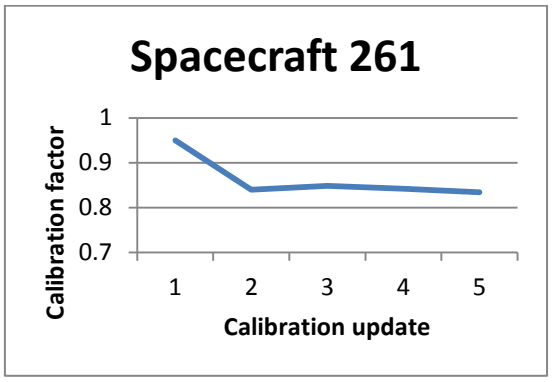

Figures 18. Calibration factors used for s/c 261 during the recovery

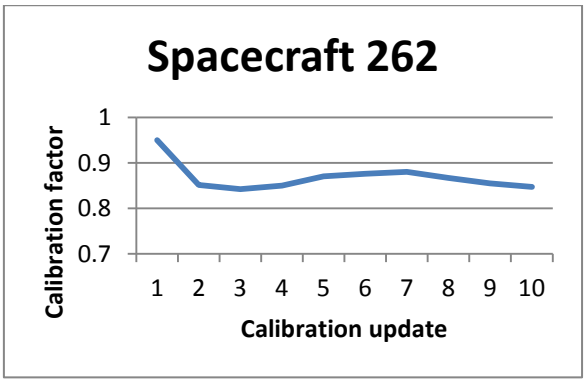

Figures 19. Calibration factors used for s/c 262 during the recovery

7.2. Off modulation

For Galileo the propulsion system activates 1 or 4 thrusters depending on the size of the manoeuvre. In case the manoeuvre with 1 thruster would take more than 0.9 seconds, then the manoeuvre is executed using the four thrusters. These four thrusters are actuated simultaneously while the attitude of the spacecraft is within certain error of depointing. In case the attitude deviates more than a certain threshold, the thrusters are switched off by pairs during an AOCS cycle in order to correct the attitude dynamically, in the so called the off modulation control.

This off modulation was evaluated as a percentage of the total manoeuvre duration for each thruster as follows:

$$\%\, Off\ modulation\ thruster = \left(1 - \frac{time\_on\_thruster}{manoeuvre\ duration}\right) \cdot 100 \tag{11}$$

During the manoeuvre campaign the average off modulation observed for both spacecraft was around a 15% at the beginning, and later on stabilized at around 10%, as can be observed in the following plots.

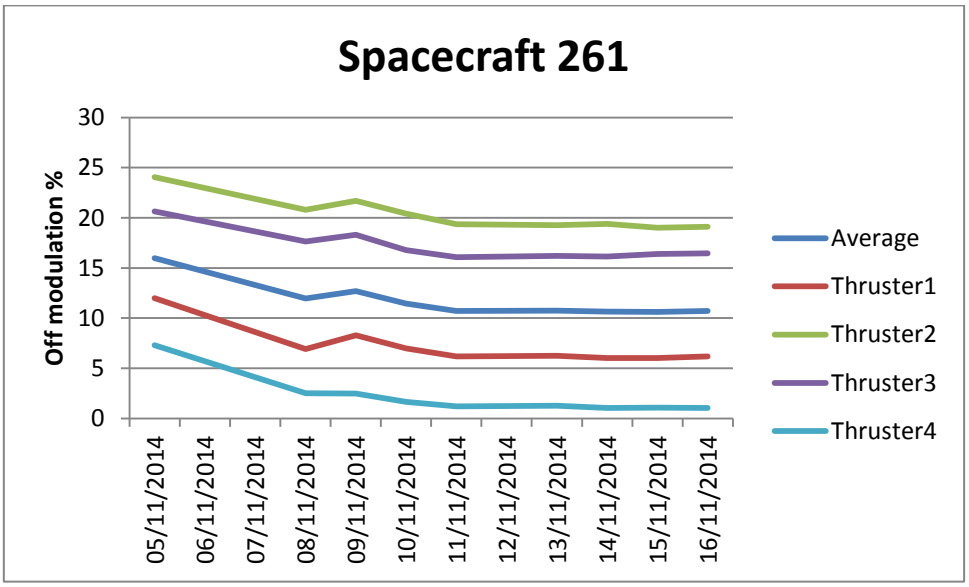

Figure 20. Off modulations observed in the manoeuvre campaign of spacecraft 261

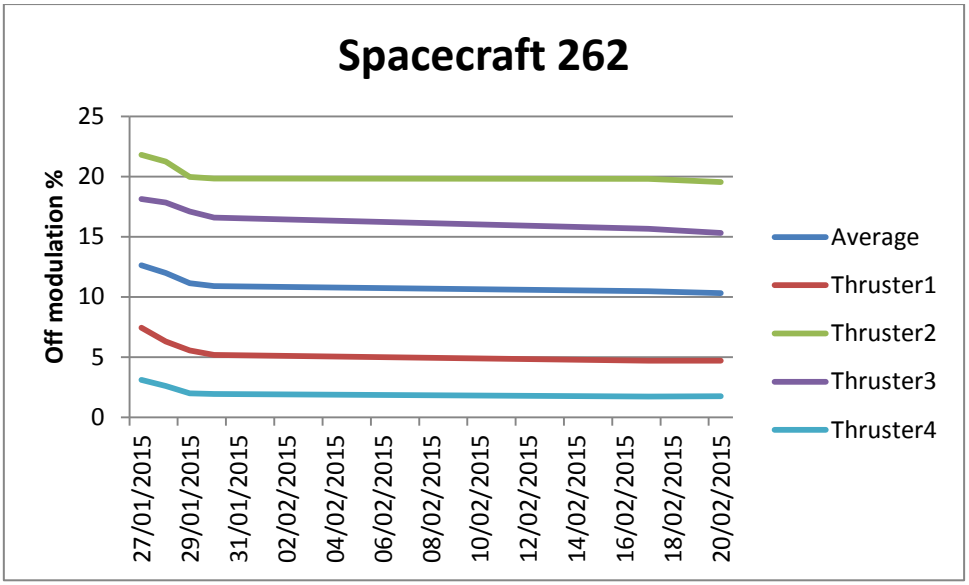

Figure 21. Off modulations observed in the manoeuvre campaign of spacecraft 262

In the beginning the pressure in the tank is higher, and therefore the force and the torques produced by the thrusters are bigger. But as long as the pressure decreases, the effect of the thruster torques decreases, so the off modulation is expected to happen with less frequency.

It is interesting to note also that the off modulation of each thruster and the average off modulation was quite stable during the manoeuvre campaign, which represented almost a complete life cycle with tank pressure decreasing from around 21 bar at the beginning until 7 bar at the end of the recovery. This points that the off modulation is quite stable in time, and can be taken into account to refine other predictions as we can see in the following section.

7.3. Correction of mass flow for the manoeuvre planning

During the manoeuvre campaign, it resulted critical to assure that the propellant budget assigned for the orbit correction was enough to reach the target orbit. For this it was necessary to refine the mass flow estimation in the manoeuvre planning model.
The telecommand system was responsible of providing the thruster performance tables to the manoeuvre planning system, which included the mass flow predictions of the thrusters for different tank filling ratios.

As the off modulation was significant during the manoeuvre execution, representing between a 10 and a 15 % manoeuvre duration, its effect was not negligible, and needed to be considered to improve the predictions of fuel mass consumption during long manoeuvres.
In order to refine the mass flow estimations, it was necessary to consider the off modulation through a off modulation factor, defined as:

$$C_{off} = \frac{\sum_i^4 time\_on\_thruster_i}{duration*4} \quad (12)$$

Where $time\_on\_thruster_i$ corresponds to the total time in which the thruster was actuating during the manoeuvre, and duration would correspond to the commanded manoeuvre duration. The corrected mass flow was then computed as the thruster model mass flow corrected by this factor:

$$\dot{m}' = C_{off} * \dot{m} \quad (13)$$

8. Conclusion

Although the nominal mission orbit could not be reached as there was not enough propellant budget to correct the injection errors, and despite of the issues related with the solar panel deployment, the LEOP and recovery phases were a success in terms of being able to deploy the solar array panels with a contingency procedure, of understanding the on board propagator behaviour in an orbit outside design specifications, and finally as it was possible to operate the two spacecraft nominally.

The experience acquired during the manoeuvre campaigns for both spacecraft may serve as well for following Galileo satellites, as almost a full life cycle could be observed in terms of propulsion actuation.

Also some of the performed analyses, such as the mass flow calibration based on the observed off modulation, gave a precedent to improve the telecommand system for other coming missions where this functionality has been implemented.

9. Acknowledgements

The authors thank the other telecommand and attitude monitoring team colleagues Cristina Santana and Audrey Clement, whose work during the LEOP and recovery also contributed to the writing of this paper, to Isidro Muñoz and Pere Ramos for assisting in the writing of this paper, and to the Galileo project for facilitating the elaboration and publication of this paper.

10. References

[1] OHB “GalileoSat FOC DI-19: Satellite Design Data and Satellite Models”

[2] OHB “GalileoSat FOC DI-19: Orbit Manoeuvre Concept”

[3] OHB “GalileoSat FOC SUM Volume 4: AOCS and Propulsion”

11. Considerations

This document has been produced under funding of the European Union. The views expressed herein can in no way be construed as reflecting the official opinion of the European Union.